HEP'99 # 7_372
Submitted to Pa 7
Pl 7, 8

DELPHI 99-89 CONF 276
15 June 1999

Search for lightest neutralino and slepton pair production in light gravitino scenarios with stau NLSP

Preliminary

DELPHI Collaboration

Paper submitted to the HEP'99 Conference
Tampere, Finland, July 15-21

Search for lightest neutralino and slepton pair production in light gravitino scenarios with stau NLSP at $\sqrt{s} = 189$ GeV

R. Alemany[(1)], F.R. Cavallo[(2)], C. García[(1)], F.L. Navarria[(2)] and G. Wolf[(3)]

(1) IFIC (Centro Mixto CSIC-Universidad de Valencia)
(2) INFN Bologna and Bologna University.
(3)CERN

Abstract

The search for promptly decaying lightest neutralinos and long-lived staus in the context of light gravitino scenarios has been updated using the 189 GeV LEP run, corresponding to an integrated luminosity of 158 pb^{-1} collected by the DELPHI experiment. In the search, it was assumed that the stau is the next to lightest supersymmetric particle (NLSP) and that the lightest neutralino is the next to NLSP (NNLSP). The search for long-lived staus has been also applied to investigate long-lived selectrons and smuons in the sleptons co-NLSP scenario. No evidence for the production of these particles was found. Hence, lower mass limits for those supersymmetric particles were set at 95% C.L.. The mass of gaugino-like neutralinos was found to be greater than 88 GeV/c^2 and that of higgsino-like neutralinos greater than 82 GeV/c^2. In the search for long-lived sleptons, lower mass limits were set as a function of the gravitino mass. Combining this search with the searches for stable heavy leptons and Minimal Supersymmetric Standard Model sleptons, lower limits on the sleptons masses were set independently of the mass of the gravitino.

1 Introduction

An update of the DELPHI results on the search for neutralino- and stau-pair production in the Gauge Mediated Supersymmetry Breaking (GMSB) scenario, using the 158 pb^{-1} integrated luminosity collected by the DELPHI experiment during 1998 is presented.

In this context, the gravitino, $\tilde{G}$, is naturally the lightest supersymmetric particle (LSP) and the next to lightest supersymmetric particle (NLSP) is unstable and decays to its Standard Model (SM) partner and a gravitino. The specific signatures of such decays depend crucially on the quantum numbers and composition of the NLSP. The number of generations of supersymmetry breaking messengers in minimal models, n, determines over most of the parameter space which particle is the NLSP [1, 2, 3, 4]. For example, for one generation of messengers, the lightest neutralino tends to be the NLSP, while for two or more generations, right-handed sleptons are favoured. Moreover, when left-right sfermion mixing [5] occurs, the corresponding $\tilde{\tau}$ state, $\tilde{\tau}_1$, becomes the NLSP. On the other hand, the $\tilde{\tau}_1$ could be nearly degenerated in mass with the other right-handed sleptons. In the case $m_{\tilde{e}} \approx m_{\tilde{\mu}} < m_{\tilde{\tau}} + m_{\tau}$, the $\tilde{e}_R$ and $\tilde{\mu}_R$ cannot have tree body decays into $\tilde{\tau}_1$ without violating lepton flavour conservation, and each of the right-handed sleptons decays only into the corresponding lepton and a gravitino, and $\tilde{\tau}_1$, $\tilde{\mu}_R$ and $\tilde{e}_R$ act effectively as co-NLSPs. The slepton lifetime depends strongly on $m_{\tilde{l}}$ and $m_{\tilde{G}}$, therefore a large variety of topologies must be investigated, in particular, the slepton could decay inside the detector.

Since the gravitino couplings are in general, with the exception of the so-called ultra-light gravitino scenarios, suppressed compared to electroweak and strong interactions, decays to the gravitino are in general only relevant for the NLSP and therefore the production and decay of supersymmetric particles at high energy colliders would generally take place through Standard Model couplings [1].

Two searches are updated here. First, $\tilde{\chi}_1^0$-pair production with the $\tilde{\chi}_1^0$ decaying into $\tilde{\tau}_1\tau$ and $\tilde{\tau}_1$ then decaying promptly into $\tau\tilde{G}$. The signature of the signal would be four τ's with missing energy and momentum from the two gravitinos (in addition to the energy and momentum carried away by the neutrinos of the decay of the τ's).

The second search concerns $\tilde{\tau}_1$-pair production followed by the decay $\tilde{\tau}_1 \rightarrow \tau\tilde{G}$ within the detector volume. The signature of such an event will be a track of a charged particle with a kink or a secondary decay vertex when the $\tilde{\tau}_1$ decays inside the tracking devices. If the decay length is too short (small $m_{\tilde{G}}$) to allow for the reconstruction of the $\tilde{\tau}_1$ track, only the decay products of the τ will be seen in the detector, and the search will then be based on track impact parameter. However, if the decay takes place outside the tracking devices (large $m_{\tilde{G}}$), the signature will be that of a heavy charged particle already studied in DELPHI [6]. For very light $m_{\tilde{G}}$ the limits from the search for Minimal Supersymmetric Standard Model (MSSM) stau can be applied [7]. All these searches have been combined to obtain a limit on $m_{\tilde{\tau}_R}$ and $m_{\tilde{\tau}_1}$ at minimal cross-section, independent of the $\tilde{G}$ mass. The $\tilde{\tau}_1$ search has been applied to $\tilde{e}_R \rightarrow e\tilde{G}$ and $\tilde{\mu}_R \rightarrow \mu\tilde{G}$ in the sleptons co-NLSP scenario to derive limits on $\tilde{e}_R$ and $\tilde{\mu}_R$ masses.

The $\tilde{\chi}_1^0$ and $\tilde{\tau}_1$ searches, together with those for $\tilde{\chi}_1^0 \rightarrow \gamma\tilde{G}$ [24] (in the $\tilde{\chi}_1^0$ NLSP scenario) and promptly decaying $\tilde{\tau}_1$-pair production [7] complement each other for different domains of the gravitino mass.

[1] One exception to this rule being the process $e^+e^- \rightarrow Z^*/\gamma^* \rightarrow \tilde{G}\tilde{\chi}_1^0$ for the case of ultra-light $\tilde{G}$ scenarios.

2 Event sample and experimental procedure

The update of the search for neutralino- and stau-pair production is based on data collected by the DELPHI experiment during 1998 at the centre-of-mass energy of 189 GeV with a total integrated luminosity of 158 pb^{-1}. A detailed description of the DELPHI detector can be found in [8] and its performance in [9].

To evaluate the signal efficiencies and background contaminations, events were generated using different programs, all relying on `JETSET` 7.4 [10], tuned to LEP 1 data [11] for quark fragmentation. The program `SUSYGEN` [12] was used to generate the neutralino-pair events and their subsequent decay products. In order to compute detection efficiencies, a total of 21000 events were generated with masses 47 GeV/$c^2 \leq m_{\tilde{\tau}_1} + 2$ GeV/$c^2 \leq m_{\tilde{\chi}_1^0} \leq \sqrt{s}/2$. A stau-pair sample of 36000 events (subdivided in 36 samples) was produced with `PYTHIA 5.7` [10] with staus having mean decay lengths from 0.25 to 200 cm and masses from m_τ to 90 GeV/c^2. Another sample of stau-pair was produced with `SUSYGEN` for the small impact parameter search with $m_{\tilde{\tau}_1} = 50, 70$ and 80 GeV/c^2. Similar samples of smuons and selectrons were produced to study the sleptons co-NLSP scenario.

The background process $\mathrm{e^+e^-} \to q\bar{q}(n\gamma)$ was generated with `PYTHIA 5.7`, while `DYMU3` [13] and `KORALZ` [14] were used for $\mu^+\mu^-(\gamma)$ and $\tau^+\tau^-(\gamma)$, respectively. The generator of reference [15] was used for $\mathrm{e^+e^-} \to \mathrm{e^+e^-}$ events.

Processes leading to four-fermion final states, $(\mathrm{Z}/\gamma)^*(\mathrm{Z}/\gamma)^*$ (where * means off-the-mass-shell), $\mathrm{W^+W^-}$, $\mathrm{We}\nu_\mathrm{e}$ and $\mathrm{Ze^+e^-}$, were also generated using `PYTHIA`. The calculation of the four-fermion background was verified using the program `EXCALIBUR` [16], which consistently takes into account all amplitudes leading to a given four-fermion final state.

Two-photon interactions leading to hadronic final states were generated using `TWOGAM` [17], separating the VDM, QPM and QCD components. The generators of Berends, Daverveldt and Kleiss [18] were used for the leptonic final states.

The cosmic radiation background was studied using the data collected before the beginning of the 1998 LEP run.

The generated signal and background events were passed through the detailed simulation [9] of the DELPHI detector and then processed with the same reconstruction and analysis programs used for real data.

3 Data selection

3.1 Neutralino pair production

The search for $e^+e^- \to \tilde{\chi}_1^0\tilde{\chi}_1^0 \to \tilde{\tau}_1\tau\tilde{\tau}_1\tau \to \tau\tilde{G}\tau\tau\tilde{G}\tau$ described in [19] was updated to include the data taken at 189 GeV applying the same selection criteria.

The data were first preselected in order to reduce low energy background (beam-gas, beam-wall, etc), $\gamma\gamma$ and large multiplicity events. The total number of simulated background events and real data events was reduced by a factor of about 6000 after applying these requirements.

The selection takes advantage of the fact that signal events can be separated into two different kinematic regions of the ($m_{\tilde{\chi}_1^0}$,$m_{\tilde{\tau}_1}$) space. The first class of events corresponds to a mass difference $\Delta m = m_{\tilde{\chi}_1^0} - m_{\tilde{\tau}_1}$ bigger than about 10 GeV/c^2. In this case all four τ's carry similar momenta. The second class of events corresponds to smaller mass

differences. In this other case the two τ's coming from the decay of the $\tilde{\tau}_1$ tend to be the most energetic, increasingly so as the $\tilde{\chi}_1^0$ mass increases. In both cases the Durham algorithm [20] was used to cluster the event in four jets by allowing y_{cut} to vary as a free variable. Numbering the jets from 1 to 4 with $E_1 > E_2 > E_3 > E_4$, a variable r was defined as:

$$r = \frac{E_3 + E_4}{E_1 + E_2} \ . \tag{1}$$

The distribution of r shifts towards lower values with increasing neutralino masses. The simulated background samples were then divided into two samples above and below $r = 0.1$ and different requirements were imposed in the two cases.

Two sets of cuts were applied in order to reduce the $\gamma\gamma$ and $f\bar{f}(\gamma)$ backgrounds and a third set of cuts to select events according to their topology:

1- The cuts against $\gamma\gamma$ backgrounds were based on the transverse energy, E_T (energy in a cone of 30° around the beam axis), missing mass and the momentum of the charged particle with largest momentum. These cuts reduced the $\gamma\gamma$ background by a factor of the order of 30.

2- The cuts against $f\bar{f}(\gamma)$ backgrounds were based on the particle multiplicity, maximum thrust, acoplanarity (after having divided the event into two jets with the Durham algorithm) and missing mass. After these cuts, the $f\bar{f}(\gamma)$ background was reduced by a factor of the order of 15.

3- The cuts based on topology take advantage of the fact that signal events tend naturally to cluster into a 4-jet topology. These jets have large polar angles and each of the four jets should be well isolated from the others.

After these cuts, an efficiency between 27 and 41% was obtained for the signal events, and the estimated background was 1.16 ± 0.19 events.

3.2 Slepton pair production

This section describes the update of the search for the process $e^+e^- \to \tilde{\tau}_1\tilde{\tau}_1 \to \tau\tilde{G}\tau\tilde{G}$ described in [21] and [19]. An additional 153.56 pb^{-1} integrated luminosity collected at the centre-of-mass energy of 189 GeV has been analysed using the same procedure as for the data collected at 183 GeV and using the same values for the data selection cuts.

Since the mean lifetime of the $\tilde{\tau}_1$ depends on the mass of the gravitino, for a gravitino with a mass of the order of a few hundred eV/c^2 or more, the stau would be sufficiently long-lived to decay outside the detector. When the mass of the gravitino is between a few eV/c^2 and a few hundred eV/c^2, one or both staus would decay in flight in some part of the detector, creating a well defined secondary vertex. The search for these decays is described in subsection 3.2.1. If the mass of the gravitino is even smaller, stau-pair production would produce displaced vertices. This search is described in subsections 3.2.2 and 3.2.3.

3.2.1 Search for secondary vertices

This analysis exploits a peculiarity of the $\tilde{\tau}_1 \to \tau\tilde{G}$ topology in the case of intermediate gravitino masses, namely, one or two tracks coming from the interaction point and at least one of them with either a secondary vertex or a kink.

Rather loose preselection cuts were imposed on the events in order to suppress the low energy background (beam-gas, beam-wall, etc), $\gamma\gamma$, e^+e^- and hadronic events. These preselection cuts left about 0.6% of the whole data sample.

The charged particle tracks of the events that survived the preselection cuts were grouped in clusters according to their first measured point (starting point). The clustering procedure is described in [22]. Each cluster contained all tracks whose starting points differed by less than 2 cm. The starting point of a cluster was defined as the average of the starting points of its tracks. This procedure allowed for clusters with a single track if its momentum was larger than 1.5 GeV/c. A cluster with only one track was considered a $\tilde{\tau}_1$ candidate if its trajectory was compatible with that of a particle coming from the interaction point (according to the selection criteria described in reference [21]) and its momentum was greater than 2 GeV/c.

For each $\tilde{\tau}_1$ candidate, a search was made for a second cluster which leading track (track of the cluster with the highest momentum) defined a crossing point with the track of the $\tilde{\tau}_1$. Such crossing point or secondary vertex was defined as the point of closest approach between the two tracks. Fake decay vertices could be present amongst the reconstructed secondary vertices, being produced by particles interacting in the detector material or by radiated photons if the particle trajectory was reconstructed into two separated tracks. These fake decay vertices were rejected if they were identified as hadronic interactions (secondary vertices reconstructed in region where there is material), if there was a radiated photon around the direction defined by the difference between the $\tilde{\tau}_1$ momentum and the momentum of the τ daughter calculated at the crossing point, or if the angle between the tracks used to define a vertex was small (less than 6°). Figure 1 shows the distribution of these quantities for real data, expected Standard Model background simulation and simulated signal for $m_{\tilde{\tau}_1} = 60$ GeV/c^2 decaying with a mean decay length of 50 cm. The excess of data in the first bins of figure 1 (c) was due to underestimation in the simulation of mismatching between the tracking devices. If no pair of tracks was found to fulfil these conditions, the event was rejected.

One event in real data was found to satisfy all the conditions described above. The event was compatible with a $\gamma\gamma \to \tau^+\tau^-$ with a hadronic interaction in the ID detector.

The vertex reconstruction procedure was sensitive to decay lengths in the xy plane, R, between 20 cm and 90 cm. Within this region a vertex was reconstructed with an efficiency of ∼52% since the VD (Vertex Detector) and the ID (Inner Detector) were needed to reconstruct the $\tilde{\tau}_1$ track and the TPC (Time Projection Chamber) to reconstruct the decay products. Inside the sensitive region the efficiency was found to be independent of the stau mass, and dropped to zero for $\tilde{\tau}_1$'s decaying near the outer surface of the TPC. The shape of the efficiency distribution was independent of the $\tilde{\tau}_1$ mass; it simply scaled down near the kinematic limit. The loss of efficiency near the kinematic limit was due to the fact that the $\tilde{\tau}_1$ boost was smaller and the vertex reconstruction less efficient when the angles between the $\tilde{\tau}_1$ and the τ products increased.

The sensitive region and the efficiency of the vertex reconstruction at 189 GeV was

slightly lower than at 183 GeV due to the loss of tracks not reconstructed with the TPC and without information in the z direction. Such tracks were not reconstructed in the 189 GeV run. However, some of the efficiency lost in the vertex search was recovered later by the search based on large impact parameter.

The efficiencies for different mean decay lengths and $\tilde{\tau}_1$ masses were calculated by applying the above selections to the simulated signal samples. For a 40 to 85 GeV/c^2 $\tilde{\tau}_1$ with mean decay length of 50 cm, the vertex search efficiency was around of 46%, decreasing near the kinematic limit, and for lower $\tilde{\tau}_1$ masses the efficiency was around 20% due to the cut for rejecting segmented tracks.

The same selection criteria was applied to smuons and selectrons. The efficiency for selectrons decreased due to the preselection cut on total electromagnetic energy (lower than $0.5\sqrt{s}$) and was around 31% for $m_{\tilde{e}_R}$ between 40 to 85 GeV/c^2, while the smuon efficiency increased to 55% for the same mass range.

3.2.2 Large impact parameter search

To investigate the region of low gravitino masses (short decay lengths) the previous search was extended to the case of the $\tilde{\tau}_1$ decaying between 0.25 cm and around 10 cm. In this case the $\tilde{\tau}_1$ track was not reconstructed and only the τ decay products were detected. The impact parameter search was only applied to those events accepted by the same general requirements as in the search for secondary vertices, and not selected by the vertex analysis. The same selection criteria described in reference [19] were applied.

The events used in this search contained exactly two single tracks with momentum larger than 1.5 GeV/c and a distance between starting points greater than 2 cm. Furthermore they were required to be acollinear (as it will be explained later) and to have large impact parameters (at least one of the two particles should have an impact parameter in the $R\phi$ projection greater than 0.2 cm).

Cosmic rays, badly reconstructed tracks or interactions in the detector material could also result in large impact parameters. However, the two tracks in a cosmic event usually had impact parameters of the same order and opposite sign (which is not the case for the signal), and the ratio between both impact parameters in the $R\phi$ projection was a clear signature of a cosmic ray event since it showed a peak at -1 while the signal was uniformly distributed. The acollinearity cut was used to reject back-to-back events with badly reconstructed tracks or interactions in the detector since they always gave small acollinearity values. Figure 2 shows the acollinearity distribution for events with two tracks in the TPC. Simulated signal events with $m_{\tilde{\tau}_1} = 60$ GeV/c^2 and a mean decay length of 2.5 cm are compared with cosmic muon events, simulated Standard Model background and real data. The data points in figure 2 contain cosmic radiation events that are not simulated. In addition, to further reduce the cosmic muon background, the acollinearity between the two tracks was requested to be smaller than 175°, since an off-time cosmic muon crossing from one TPC drift sector to another was reconstructed as two almost parallel tracks. This cosmic ray background is shown in figure 2 but it is not taken into account when computing limits.

The efficiencies were derived for the different $\tilde{\tau}_1$ masses and decay lengths by applying the same selection to the simulated signal events. The maximum efficiency was 32% corresponding to a mean decay length of 2.5 cm. The efficiency decreased very fast for

lower decay lengths due to the cut on minimum impact parameter. The efficiency at 189 GeV was slightly larger than at 183 GeV since some events not passing the secondary vertex selection were recovered in this search, as explained before. For longer decay lengths, the appearance of reconstructed $\tilde{\tau}_1$ tracks in combination with the cut on the maximum amount of charged particle tracks caused the efficiency to decrease smoothly. This decrease is compensated by a rising efficiency in the search for secondary vertices. For masses above 30 GeV/c^2 no dependence on the $\tilde{\tau}_1$ mass was found far from the kinematic limit. However for lower masses the efficiency decreased and it was almost zero for a 5 GeV/c^2 $\tilde{\tau}_1$.

The same selection was applied to selectrons and smuons. For smuons the efficiency increased to 59% for a mean decay length of 2.5 cm and masses over 30 GeV/c^2 since the smuon have always one prompt decay. For selectrons the efficiencies were almost the same that for staus.

Trigger efficiencies were studied simulating the DELPHI trigger response to the events selected by the vertex search and by the large impact parameter analysis, and were found to be around 99%.

No events in the real data sample were selected with the above criteria. The number of expected background events at $\sqrt{s} = 189$ GeV is shown in Table 1 for the combination of the vertex and large impact parameter searches.

Observed events	1
Total background	$1.42^{+0.72}_{-0.36}$
$Z^*/\gamma \to (ll)(n\gamma)$	$0.23^{+0.35}_{-0.01}$
4-fermion (except $\gamma\gamma$)	0.45±0.16
$\gamma\gamma \to \tau^+\tau^-$	$0.74^{+0.59}_{-0.32}$

Table 1: Number of observed events at $\sqrt{s} = 189$ GeV, together with the total number of expected background events and the expected numbers from the individual background sources, for both large impact parameter and secondary vertex searches combined.

3.2.3 Small impact parameter search

The large impact parameter search can be extended further down to mean decay lengths of around 0.1 cm. The same selection criteria described in reference [19] was applied. However, some extra selection was added in order to reduce background from detector noise or failure, cosmic radiation and $\tau\tau$ events.

Events with anomalous noise in the TPC were rejected requiring less than 20 charged particles (before track selection) and relative error of the measured momentum of the leading tracks (charged particles with larger momentum in each hemisphere) less than 50%. The cosmic muon rejection was improved by requiring that the leading tracks with impact parameters larger than 1 cm must be reconstructed in the TPC. To reduce the $\tau\tau$ events with 1-3 topology (when the single track is not reconstructed), and also gamma

conversions, any leading track must have at least other charged particle at an angular distance larger 5°.

The efficiency of the search turned out not to depend on the $\tilde{\tau}_1$ mass for masses over 40 GeV/c^2, but rather on the $\tilde{\tau}_1$ decay length in the laboratory system. The maximum efficiency was $\sim$ 38% for a mean decay length of $\sim$ 2 cm, the efficiency dropped at small decay lengths ($\sim$ 15% at 1 mm).

The same selection criteria were used to search for smuons. To search for selectrons, in order to increase efficiency, the cut $(E_1 + E_2) < 0.7$ (where E_1, E_2 are the electromagnetic energy deposits associated to the leading tracks) was not applied. The Bhabha events that survived the selection, when the previous rejection cut was not applied, were those where at least one of the electrons underwent a secondary interaction, thus acquiring a large impact parameter. However, it was found that in these cases the measured momentum of the electron was smaller than the electromagnetic energy deposition around the electron track. Therefore, the cut $(E_1/p_1 + E_2/p_2) < 2.2$ was used for the selectron search. The maximum efficiency reach for the smuon search was 43% and for the selectron search 35% at 2 cm mean decay length.

The number of events selected in data was 4, and $4.54^{+1.12}_{-0.57}$ events were expected from Standard Model background (see table 2). Two of the candidates had tracks with fitting problems and the other two events were compatible with Standard Model $\tau\tau$ events.

Observed events	4
Total background	$4.54^{+1.12}_{-0.57}$
$Z^*/\gamma \to (\tau\tau)(n\gamma)$	$1.33^{+0.46}_{-0.35}$
$\gamma\gamma \to \tau^+\tau^-$	$0.61^{+0.99}_{-0.38}$
WW	$2.52^{+0.26}_{-0.23}$
ZZ	$0.08^{+0.04}_{-0.03}$

Table 2: Expected simulated SM background events and selected data events at 189 GeV centre-of-mass energy for the small impact parameter search.

4 Results and interpretation

4.1 Neutralino pair production

One event was observed to pass the neutralino search at $\sqrt{s} = 189$ GeV and 1.16 ± 0.19 background events were expected.

Since no evidence for a signal was found in the data, a limit on the production cross-section for neutralino-pair was derived for each $(m_{\tilde{\chi}^0_1}, m_{\tilde{\tau}_1})$ combination. A statistical error of $\pm 1.5\%$ was assumed for the signal efficiency.

In what follows, the model described in reference [2] will be used in order to derive limits. This is a general model which assumes only radiatively broken electroweak symmetry and null trilinear couplings at the messenger scale. The corresponding parameter space was scanned as follows: $1 \leq n \leq 4$, 5 TeV $\leq \Lambda \leq$ 900 TeV, $1.1 \leq M/\Lambda \leq 9000$, $1.1 \leq \tan\beta \leq 50$, and $\mu > 0$, where n is the number of messenger generations in the

model, Λ is the ratio between the vacuum expectation values of the auxiliary component superfield and the scalar component of the superfield and M is the messenger mass scale. The parameters tan β and μ are defined as for the MSSM.

Figure 3 shows the 95% C.L. upper limit for the $\tilde{\chi}_1^0$-pair production cross-section at $\sqrt{s} = 189$ GeV as a function of $m_{\tilde{\chi}_1^0}$ and $m_{\tilde{\tau}_1}$ after combining the results of the searches at $\sqrt{s} = 161$, 172 183 and 189 GeV with the maximum likelihood ratio method [23]. For different number of messenger generations, the ratios between production cross sections at different energies are bound to vary within certain limits. The same happens when considering scenarios with higgsino- or gaugino-like neutralinos. Figure 3 presents as an example the case of $n = 3$ and gaugino-like $\tilde{\chi}_1^0$. For the other scenarios considered in this study ($1 \leq n \leq 4$, and gaugino- or higgsino-like neutralinos), the maximum difference with respect to figure 3 occurs in the region where $m_{\tilde{\chi}_1^0} < 80$ GeV/c^2 and $m_{\tilde{\tau}_1} < 65$ GeV/c^2, and is not bigger than 10%.

Given the aforementioned limits for the production cross-section, some sectors of the $(m_{\tilde{\chi}_1^0}, m_{\tilde{\tau}_1})$ space can be excluded. In order to achieve the maximum sensitivity, the results from two other analyses are taken into account. The first is the search for $\tilde{\tau}_1$-pair production in the context of the MSSM. In the case where the MSSM $\tilde{\chi}_1^0$ is massless, the kinematics corresponds to the case of $\tilde{\tau}_1$ decaying into a τ and a gravitino, except for spin effects, which are not taken into account in SUSYGEN. The second is the search for lightest neutralino-pair production in the region of the mass space where $\tilde{\chi}_1^0$ is the NLSP [24] (the region above the diagonal line, i.e. $m_{\tilde{\tau}} > m_{\tilde{\chi}_1^0}$). Within this zone, the neutralino decays into a gravitino and a photon.

As an illustration, fig. 4 presents the 95% C.L. excluded areas for the case $n = 2$ and gaugino-like neutralinos in the $m_{\tilde{\chi}_1^0}$ *vs.* $m_{\tilde{\tau}_1}$ plane. The positive-slope dashed area is excluded by this analysis. The resulting 95% C.L. lower limit for the mass of the lightest neutralino is 88 GeV/c^2. The negative-slope dashed area is excluded by the analysis searching for neutralino-pair production followed by the decay $\tilde{\chi}_1^0 \to \tilde{G}\gamma$. The point-hatched area is excluded by the direct search for MSSM $\tilde{\tau}_1$-pair production [7], taking into account the possibility of $\tilde{\tau}_L - \tilde{\tau}_R$ mixing [5].

For other cases, lower limits for the mass of the lightest neutralino obtained with this analysis are described in table 3. In the case of $n = 1$ and gaugino-like lightest neutralino, the NLSP is always the $\tilde{\chi}_1^0$, and the lower limit is derived from the search for acoplanar photons [24].

n	gaugino-like $\tilde{\chi}_1^0$ (GeV/c^2)	higgsino-like $\tilde{\chi}_1^0$ (GeV/c^2)
1	91.	82.
2	88.	85.
3	88.	85.
4	88.	85.

Table 3: The 95% C.L. lower limits for $m_{\tilde{\chi}_1^0}$ for eight different scenarios. When $n = 1$ and the lightest neutralino is gaugino-like, the limit comes from the search for two acoplanar photons.

4.2 Slepton pair production

One candidate was observed to pass the selection of the secondary vertex search and the total number of background events expected was $1.42^{+0.72}_{-0.36}$ (combining vertex and large impact parameter searches). The event was compatible with a hadronic interaction in a $\gamma\gamma \to \tau\tau$ event. Four candidates were observed to pass the small impact parameter search and $4.54^{+1.12}_{-0.57}$ events were expected from Standard Model background. The results of these analyses were combined with those of the stable heavy lepton search described in [6], which considers that the $\tilde{\tau}_1$ decays outside the tracking devices ($R > 200$ cm). For very large $\tilde{\tau}_1$ masses, efficiencies around 67% were obtained by the stable heavy lepton search. As an event could be selected both by the vertex search and by the stable heavy lepton search, there is a correlation which was also considered.

Figure 5 shows the 95% C.L. upper limit for the $\tilde{\tau}_1$-pair production cross-section at $\sqrt{s} = 189$ GeV after combining the results of the searches at $\sqrt{s} = 130 - 189$ GeV with the maximum likelihood ratio method [23]. The results are presented in the ($m_{\tilde{G}}$,$m_{\tilde{\tau}_1}$) plane combining the two impact parameter searches, the secondary vertex analysis and the stable heavy lepton search. The minimum upper limits achieved for a given $\tilde{\tau}_1$ were around 0.05-0.10 pb depending on $m_{\tilde{G}}$. For $m_{\tilde{G}} > 9$ eV/c^2 and a 80.0 GeV/c^2 $\tilde{\tau}_1$, a 0.10 pb limit was obtained. Figure 6 shows the 95% C.L. upper limit for the $\tilde{\mu}_R$- and $\tilde{e}_R$-pair production cross-sections. Assuming mass degeneracy of the three supersymmetric particles, $\tilde{\tau}_1$, $\tilde{e}_R$ and $\tilde{\mu}_R$, Figure 6 (bottom plot) shows the 95% C.L. upper limit for the $\tilde{l}_R$-pair production cross-section.

The upper limits for the $\tilde{\tau}_1$-pair production cross-section were interpreted in the framework of $\tilde{\tau}_1$ NLSP scenario to exclude $m_{\tilde{\tau}_1}$ values as a function of $m_{\tilde{G}}$ combining all LEP2 energies (Figure 7 upper plot). The large impact parameter and secondary vertex analyses allow the exclusion of $\tilde{\tau}_1$ with a mass below 80 GeV/c^2 for gravitino masses between 10 and 310 eV/c^2, and with a mass below 84 GeV/c^2 for gravitino masses between 70 and 250 eV/c^2, at 95% C.L.. For $\tilde{G}$ larger than 1000 eV/c^2 the limit was 86.1 GeV/c^2 obtained from the stable heavy lepton search [6]. Near the mixing angle which gives the minimum $\tilde{\tau}_1$-pair production cross-section, due to the vanishing coupling to the Z no limit can be inferred from the LEP1 measurements, therefore the search was extended to stau masses around m_τ. Masses below m_τ were excluded from the stable $\tilde{\mu}$ search in JADE [26].

In the sleptons co-NLSP scenario the results obtained were the following. The cross-section limits of Figure 5 were used to exclude right-handed stau masses (Figure 7 bottom plot) as a function of the gravitino mass. The cross-section limits of Figure 6 were used to derive limits for right-handed smuons (Figure 8 upper plot) and right-handed selectrons (Figure 8 middle plot) at 95% C.L.. For selectrons the production cross-section was calculated neglecting contributions from the t–channel process. Assuming that the three sleptons have the same mass, lower limits for this mass were derived as can be seen in Figure 8 (bottom plot), where for very short lifetimes only $\tilde{\mu}_R$ was considered since it is the best limit that can be achieved in absence of slepton combination. Therefore, in the framework of sleptons co-NLSP, the impact parameter search and the secondary vertex search allow the exclusion of $\tilde{\tau}_R$ masses below 80 GeV/c^2 for gravitino masses between 8 and 380 eV/c^2, and below 84 GeV/c^2 for gravitino masses between 15 and 380 eV/c^2. For the case of $\tilde{\mu}_R$, masses below 80 GeV/c^2 for gravitino masses between 15 and 370 eV/c^2, and below 84 GeV/c^2 for gravitino masses between 23 and 310 eV/c^2, are excluded. And finally, for the case of $\tilde{e}_R$, masses below 80 GeV/c^2 for gravitino masses between

12 and 301 eV/c^2, and masses below 84 GeV/c^2 for gravitino masses between 28 and 260 eV/$c^2$are excluded. And assuming slepton mass degeneracy, these searches exclude $\tilde{l}_R$ masses below 84 GeV/c^2 for $\tilde{G}$ masses between 9 and 570 eV/c^2 and below 90 GeV/c^2 for $\tilde{G}$ masses between 40 and 380 eV/c^2, at 95% C.L.. For $\tilde{G}$ larger than 1000 eV/c^2 the limit was 86.1 GeV/c^2 obtained from the stable heavy lepton search [6]. $\tilde{l}_R$ masses below 35 GeV/c^2 are excluded from the Z invisible decay width [25].

5 Summary

Lightest neutralino- and slepton-pair production were searched for in the context of light gravitino scenarios. In what concerns the NLSP, two scenarios were explored: the $\tilde{\tau}_1$ NLSP and the $\tilde{l}_R$ co-NLSP scenarios. The NNLSP was the $\tilde{\chi}_1^0$.

The search for neutralino-pair production produced one candidate event to be compared to 1.16±0.19 events expected from the SM background for $\sqrt{s}$ = 189 GeV. An upper limit for the corresponding production cross-section between 0.070 and 0.085 pb was set at 95% C.L. in the kinematically allowed region. The DELPHI collaboration sets a lower limit for the mass of the $\tilde{\chi}_1^0$ at 82 GeV/c^2 at 95% C.L..

The search for pair production of long-lived staus produced one candidate for the secondary vertex and large impact parameter methods, and four for the small impact parameter method, whereas totals of $1.42^{+0.72}_{-0.36}$ and $4.54^{+1.12}_{-0.57}$ events were expected from the simulated SM background, respectively. An upper limit for the stau-pair production cross-section was set as a function of its mass and that of the gravitino, between 0.05 and 2 pb at 95% C.L. in the kinematically allowed region. In the framework of $\tilde{\tau}_1$ NLSP scenario, this result, together with the search for staus within the MSSM framework and stable stau production, allow the DELPHI collaboration to set a lower limit for the mass of the $\tilde{\tau}_1$ at 73 GeV/c^2 at 95% C.L..

The stau search was applied to smuons and selectrons. In the framework of $\tilde{l}_R$ co-NLSP scenario, which assumes mass degeneracy between the right-handed sleptons, the combination of the impact parameter methods, secondary vertex search, stable sleptons search and the search for sleptons in the MSSM scenario, allows the DELPHI collaboration to set a lower limit for the masses of the $\tilde{l}_R$ at 79 GeV/c^2 at 95% C.L. irrespective of the gravitino mass.

References

[1] J. A. Bagger, K. Matchev, D. M. Pierce and R. Zhang, Phys. Rev. **D55** (1997) 3188.

[2] D. A. Dicus, B. Dutta, S. Nandi, Phys. Rev. **D56** (1997) 5748 ;
D. A. Dicus, B. Dutta, S. Nandi, Phys. Rev. Lett. **78** (1997) 3055.

[3] F. Borzumati, *On the Minimal Messenger Model*, hep-ph/9702307.

[4] G.F. Giudice, R. Rattazzi, *Theories with Gauge-Mediated Supersymmetry Breaking*, hep-ph/9801271, Submitted to Phys. Rev. D.

[5] A. Bartl *et. al.*, Z. Phys. C73(1997) 469.

[6] DELPHI Collaboration, P. Abreu *et al.*, Phys. Lett. **B444** (1998) 491;
DELPHI 99-75 CONF 262, contribution # 7-119 to HEP99.

[7] DELPHI 99-78 CONF 265, contribution # 7-230 to HEP99.

[8] DELPHI Collaboration, P. Aarnio et al., Nucl. Instr. and Meth. **303** (1991) 233.

[9] DELPHI Collaboration, P. Abreu et al.,Nucl. Instr. and Meth. **378** (1996) 57.

[10] T. Sjöstrand, Comp. Phys. Comm. **39** (1986) 347;
T. Sjöstrand, `PYTHIA 5.6` *and* `JETSET 7.3`, CERN-TH/6488-92.

[11] DELPHI Collaboration, P. Abreu *et al.*, Z. Phys. **C73** (1996) 11.

[12] SUSYGEN 2.12, S. Katsanevas and S. Melachroinos in *Physics at LEP2*, CERN 96-01, Vol. 2, p. 328 and http://lyohp5.in2p3.fr/delphi/katsan/susygen.html .

[13] J.E. Campagne and R. Zitoun, Z. Phys. **C43** (1989) 469.

[14] S. Jadach and Z. Was, Comp. Phys. Comm. **79** (1994) 503.

[15] F.A. Berends, R. Kleiss, W. Hollik, Nucl. Phys. **B304** (1988) 712.

[16] F.A. Berends, R. Pittau, R. Kleiss, Comp. Phys. Comm. **85** (1995) 437.

[17] S. Nova, A. Olshevski, and T. Todorov, *A Monte Carlo event generator for two photon physics*, DELPHI note 90-35 (1990).

[18] F.A. Berends, P.H. Daverveldt, R. Kleiss, Comp. Phys. Comm. **40** (1986) 271, Comp. Phys. Comm. **40** (1986) 285, Comp. Phys. Comm. **40** (1986) 309.

[19] DELPHI Collaboration, P. Abreu *et al.*, E. Phys. J. C7 (1999) 595.

[20] S. Catani, Phys. Lett. **B269** (1991) 432 .

[21] DELPHI Collaboration, P. Abreu *et al.*, E. Phys. J. C6 (1999) 385.

[22] DELPHI Collaboration, P. Abreu *et al.*, Zeit. Phys. C74 (1997) 57.

[23] A.L. Read, *Optimal statistical analysis of search results based on the likelihood ratio and its application to the search for the MSM Higgs boson at* $\sqrt{s} = 161$ *and 172 GeV*, DELPHI 97-158 PHYS 737 (1997) and references therein.

[24] DELPHI Collaboration, P. Abreu *et al.*, E. Phys. J. C6 (1999) 371;
DELPHI 99-15 CONF 215.

[25] ALEPH Collaboration, R. Barate *et al.*, Phys. Lett. B407 (1997) 377;
The LEP and SLD Collaborations, J Alcaraz *et al.*, CERN-PPE/96-183,

[26] JADE Collaboration, W. Bartel *et al.*, Phys. Lett. B152 (1985) 392.

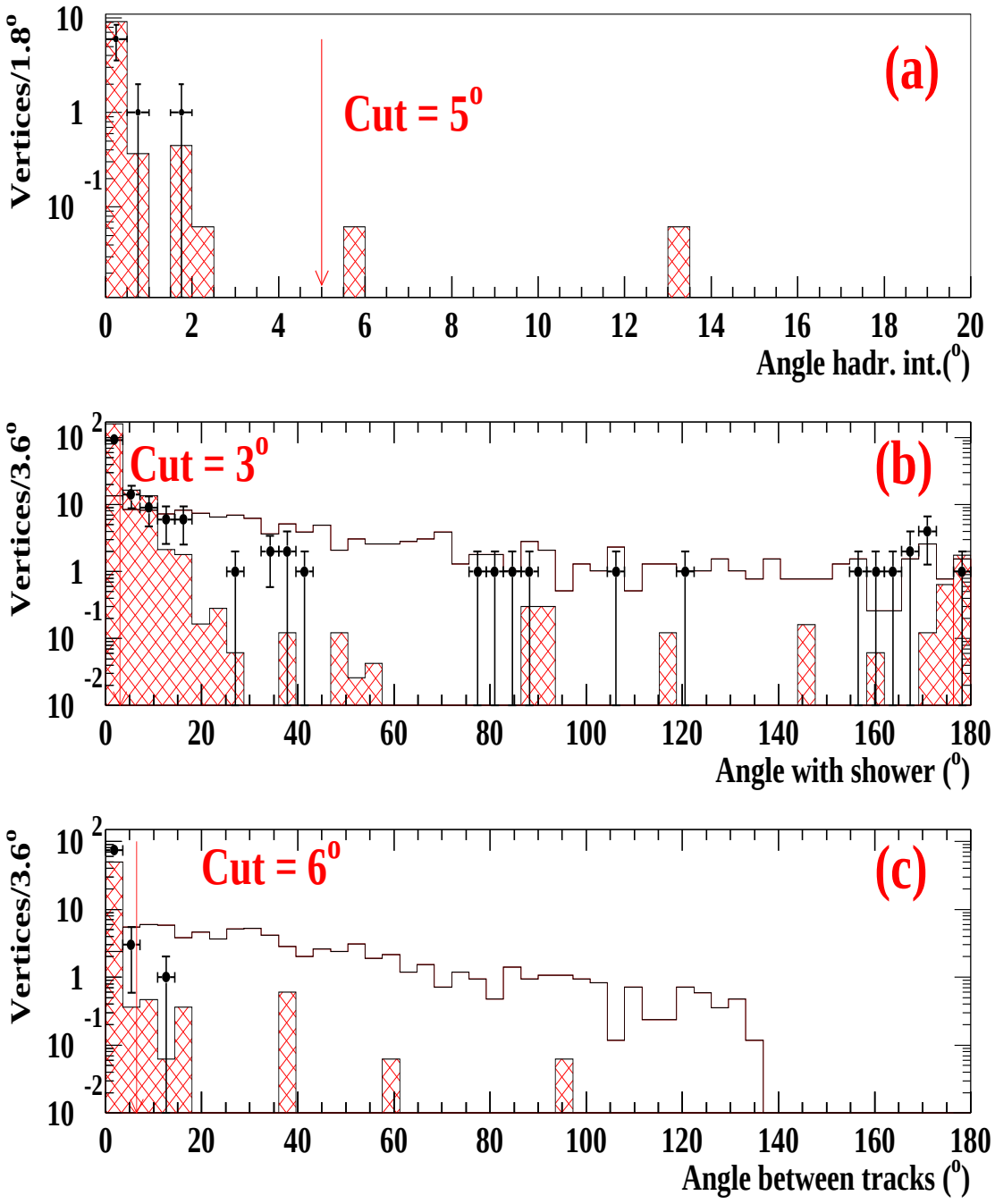

Figure 1: (a) angle between the hadronic interaction and the reconstructed vertex, (b) angle between the electromagnetic shower and the direction defined by the difference between the momenta of $\tilde{\tau}_1$ and its associated τ_d, defined at the crossing point, and (c) angle between the tracks of the kink, for real data (dots), expected Standard Model background (cross-hatched histogram) and simulated signal for $m_{\tilde{\tau}_1} = 60$ GeV/c^2 decaying with a mean distance of 50 cm (blank histogram). The arrows indicate the selection criteria imposed.

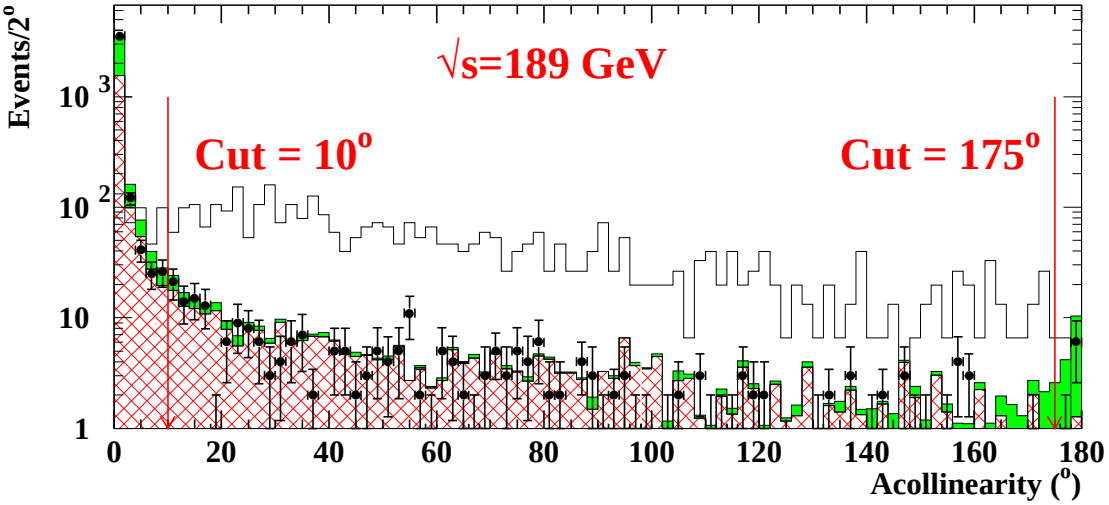

Figure 2: Acollinearity for real data (dots), a simulated signal of $m_{\tilde{\tau}_1} = 60$ GeV/c^2 decaying with a mean distance of 2.5 cm (blank histogram), and expected simulated Standard Model background (cross-hatched histogram) plus cosmic background (dark grey histogram). This last background is normalised so as to make the first bin of SM background plus cosmic radiation coincide with the corresponding value for the real data. The selection on this variable is shown with arrows.

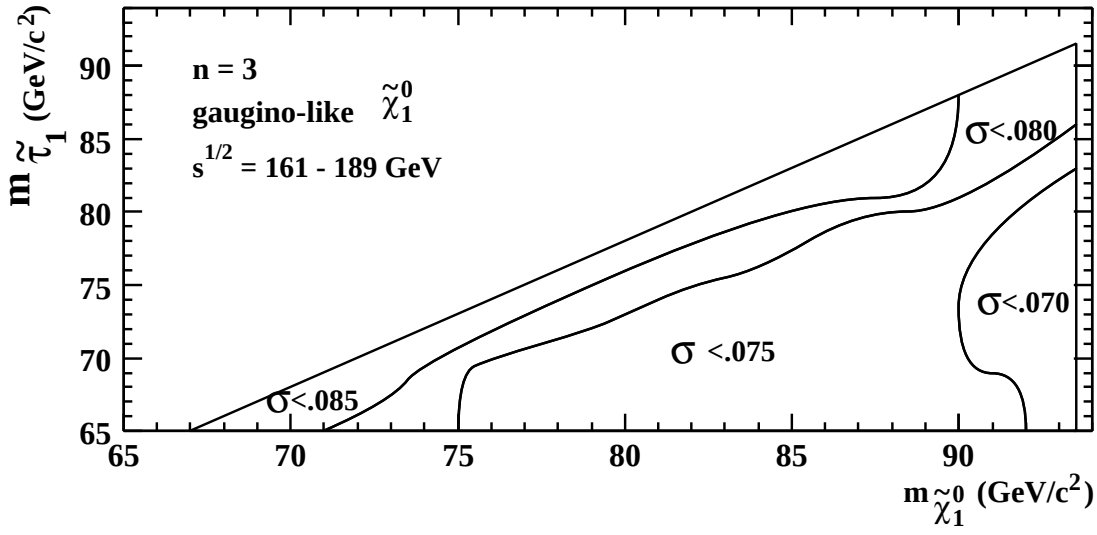

Figure 3: 95% C.L. upper limit of the $\tilde{\chi}_1^0$-pair production cross-section (in picobarn) at $\sqrt{s} = 189$ GeV after combining the results of the searches at $\sqrt{s} = 161$, 172 183 and 189 GeV, as a function of $m_{\tilde{\chi}_1^0}$ and $m_{\tilde{\tau}_1}$ for the case $n = 3$ and gaugino-like neutralinos, where n is the number of messenger generations. The diagonal and vertical lines show respectively the limits $m_{\tilde{\chi}_1^0} = m_{\tilde{\tau}} + m_{\tau}$ and $m_{\tilde{\chi}_1^0} = \sqrt{s}/2$.

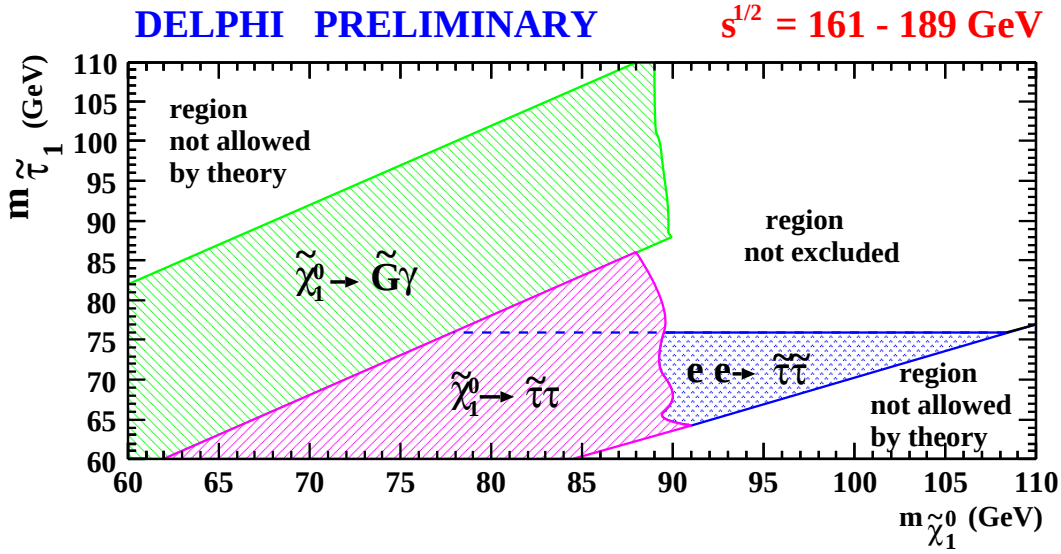

Figure 4: Areas excluded at 95% C.L. for $n = 2$, gaugino-like neutralinos and $m_{\tilde{G}} < 1$ eV/c^2 in the $m_{\tilde{\chi}_1^0}$ *vs.* $m_{\tilde{\tau}_1}$ plane. The positive-slope dashed area is excluded by this analysis. The negative-slope dashed area is excluded by the search for $\tilde{\chi}_1^0 \to \gamma\tilde{G}$, and the point-hatched area by the direct search for stau-pair production in the MSSM framework.

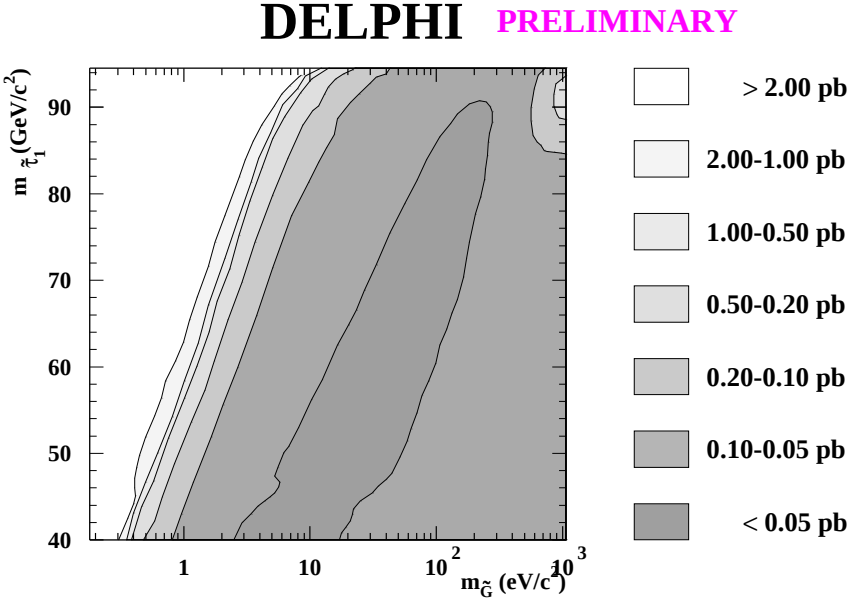

Figure 5: 95% C.L. upper limit of the $e^+e^- \to \tilde{\tau}_1\tilde{\tau}_1$ production cross-section at $\sqrt{s}$=189 GeV after combining the results of the searches at $\sqrt{s} = 130-189$ GeV. Results are shown in the ($m_{\tilde{G}}$,$m_{\tilde{\tau}_1}$) plane. Searches for events containing charged particle tracks with small impact parameter, large impact parameter, secondary vertices and the search for heavy stable leptons are combined.

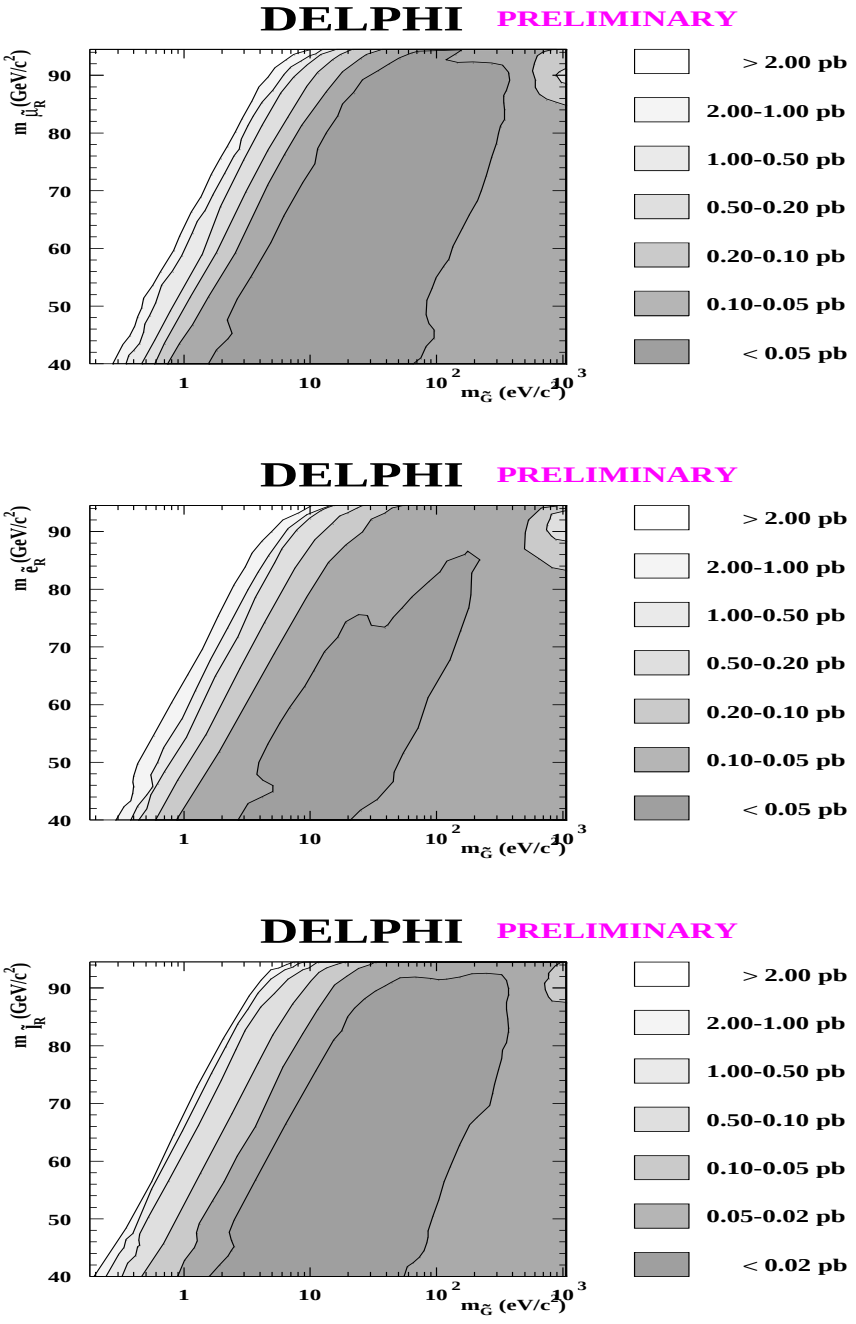

Figure 6: 95% C.L. upper limit of the $e^+e^- \to \tilde{\mu}_R\tilde{\mu}_R$ (upper plot), $e^+e^- \to \tilde{e}_R\tilde{e}_R$ (middle plot) and $e^+e^- \to \tilde{l}_R\tilde{l}_R$ (bottom plot) production cross-sections at $\sqrt{s} = 189$ GeV after combining the results of the searches at $\sqrt{s} = 130{-}189$ GeV. Searches for events containing charged particles tracks with small impact parameter, large impact parameter, secondary vertices and the search for heavy stable leptons are combined.

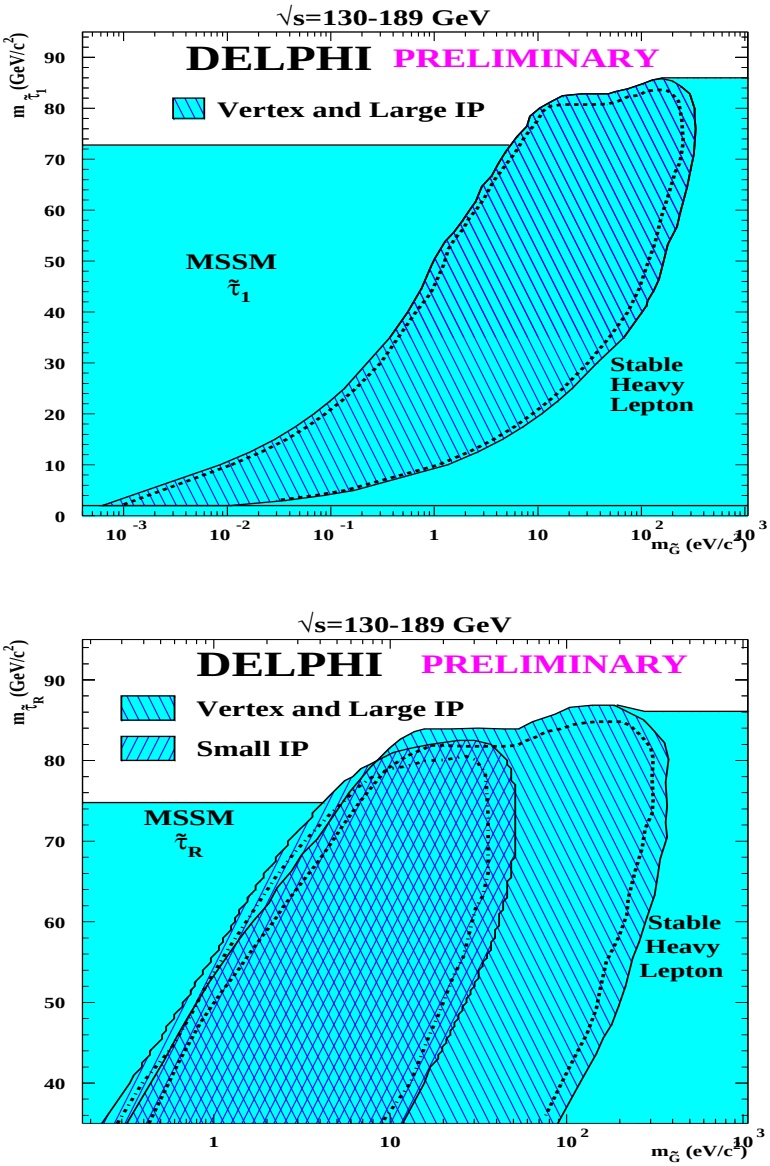

Figure 7: Exclusion region in the ($m_{\tilde{G}}$,$m_{\tilde{\tau}_1}$) (upper plot) plane and ($m_{\tilde{G}}$,$m_{\tilde{\tau}_R}$) plane (bottom plot) at 95% C.L. for the present analysis combined with the stable heavy lepton search and the MSSM $\tilde{\tau}_1$ search, using all LEP-2 data. The positive-slope hatched area shows the region excluded by the small impact parameter search. The negative-slope hatched area shows the region excluded by the combination of the large impact parameter and secondary vertex searches. The dashed line shows the expected limits.

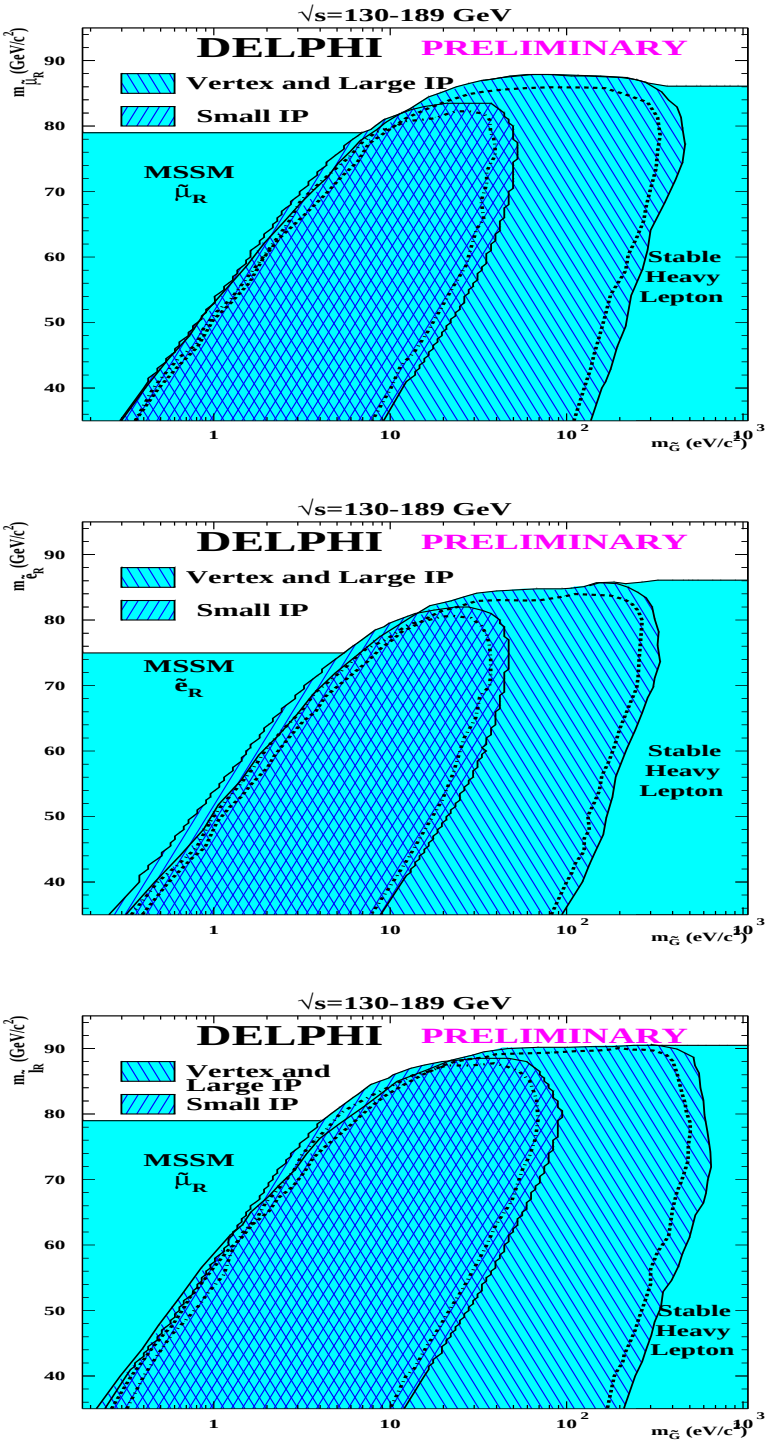

Figure 8: Exclusion regions in the ($m_{\tilde{G}}$,$m_{\tilde{\mu}_R}$) (upper plot), ($m_{\tilde{G}}$,$m_{\tilde{e}_R}$) (middle plot) and ($m_{\tilde{G}}$,$m_{\tilde{l}_R}$) (bottom plot) planes at 95% C.L. for the present analysis combined with the stable heavy lepton search and the MSSM $\tilde{\tau}_R$ search, using all LEP-2 data. The positive-slope hatched area shows the region excluded by the small impact parameter search. The negative-slope hatched area shows the region excluded by the combination of the large impact parameter and secondary vertex searches. The dashed line shows the expected limits. For $\tilde{e}_R$ only the contribution of s–channel has been considered.